Nature Metabolism – Perspective
Manuscript in preparation for re-submission; version 0.6 (2020-05-07)

Mitochondrial respiratory states and rates

Gnaiger Erich et al (MitoEAGLE Task Group)*

Corresponding author: Erich Gnaiger
Chair COST Action CA15203 MitoEAGLE – http://www.mitoeagle.org
Department of Visceral, Transplant and Thoracic Surgery, D. Swarovski Research Laboratory, Medical University of Innsbruck, Innrain 66/4, A-6020 Innsbruck, Austria
Email: mitoeagle@i-med.ac.at; *Tel: +43 512 566796, Fax: +43 512 566796 20*

Running title: Mitochondrial states and rates

As the knowledge base and importance of mitochondrial physiology to evolution, health, and disease expands, the necessity for harmonizing the terminology concerning mitochondrial respiratory states and rates has become increasingly apparent. The chemiosmotic theory establishes the mechanism of energy transformation in oxidative phosphorylation (OXPHOS) and provides the theoretical foundation of mitochondrial physiology and bioenergetics. We follow guidelines of the International Union of Pure and Applied Chemistry (IUPAC) on terminology, extended by considerations of mitochondrial respiratory control, metabolic flows and fluxes. The OXPHOS-capacity is respiration measured at kinetically-saturating concentrations of ADP and inorganic phosphate. The oxidative electron transfer-capacity reveals the possible limitation of OXPHOS-capacity mediated by the phosphorylation-pathway and is measured as noncoupled respiration at optimum concentrations of external uncouplers. LEAK-respiration is the intrinsically uncoupled oxygen consumption, compensating mainly for ion leaks — particularly the proton leak — and studied in the absence of ADP or by inhibition of the phosphorylation-pathway. Uniform standards for evaluation of respiratory states and rates will ultimately contribute to reproducibility between laboratories and thus support the development of databases of mitochondrial respiratory function in species, tissues, and cell types. Clarity of concept and consistency of nomenclature facilitate effective transdisciplinary communication, education, and ultimately further discovery.

Keywords: Mitochondrial respiratory control, coupling control; mitochondrial preparations; protonmotive force; uncoupling; oxidative phosphorylation: OXPHOS; electron transfer: ET; electron transfer system: ETS; proton leak, ion leak and slip compensatory state: LEAK; residual oxygen consumption: ROX; State 2; State 3; State 4; normalization; flow; flux; oxygen: O_2

Harmonization of nomenclature

Mitochondria are essential cellular, membrane-enclosed organelles that perform a large range of functions critical for cell viability. Their best-known function is to synthesize adenosine triphosphate (ATP) via oxidative phosphorylation (OXPHOS), but they also have important functions related to cellular metabolism and cell-signalling. This importance has led to a large and increasing body of research devoted to better understanding mitochondrial respiratory function. However, the dissemination of fundamental knowledge and implementation of novel discoveries require communication with a commonly understood terminology. Reproducibility of experimental procedures also depends on strictly-defined conditions and harmonization of shared research protocols. Unfortunately, a consensus on nomenclature and conceptual coherence is currently missing in the expanding field of mitochondrial physiology and bioenergetics. The use of sometimes vague, ambiguous, or inconsistent terminology likely contributes to confusion, miscommunication, and the

conversion of valuable signals to wasteful noise. Thus, complementary to quality control a conceptual framework is required to standardise and harmonise terminology and methodology.

To fill the current gap, this perspective aims to harmonize nomenclature and addresses the terminology on coupling states and fluxes through metabolic pathways of aerobic energy transformation in mitochondrial (mt) preparations. In an attempt to establish a transdisciplinary nomenclature, we strive to incorporate a concept-driven terminology of bioenergetics with explicit, easily recognized terms and symbols that define mitochondrial respiratory states and rates. The consistent use of terms and symbols will facilitate transdisciplinary communication for quantitative modelling and data repositories on bioenergetics and mitochondrial physiology. [1-3]

Coupling in mitochondrial respiration

Respiration and fermentation. Aerobic respiration is the O_2 flux in (*1*) OXPHOS with catabolic reactions leading to O_2 consumption coupled to phosphorylation of ADP to ATP, plus (*2*) O_2 consuming reactions apart from OXPHOS. Coupling of electron transfer (ET) to ADP→ATP phosphorylation is mediated by vectorial translocation of protons across the mitochondrial inner membrane (mtIM). Proton pumps generate or utilize the electrochemical protonmotive force, *pmF* (Fig. 1). The *pmF* is the sum of two partial forces, the electric force (electric potential difference) and chemical force (proton chemical potential difference, related to ΔpH). [4,5] Cell respiration is thus distinguished from fermentation: (*1*) Compartmental coupling in vectorial OXPHOS[4,5] contrasts to substrate-level phosphorylation in fermentation without utilization of O_2. (*2*) Redox balance is maintained in aerobic respiration by O_2 as the electron acceptor supplied externally, whereas fermentation is characterized by internal electron acceptors formed in intermediary metabolism (Fig. 1a).

Respiratory states and respiratory capacity. Cell membranes include organellar membranes and the plasma membrane, which separates the intracellular milieu from the extracellular environment (Fig. 1a). The plasma membrane consists of a lipid bilayer with embedded proteins and attached organic molecules that collectively control the selective permeability of ions, organic molecules and particles, limiting the passage of many water-soluble mitochondrial substrates and inorganic ions. Such limitations are overcome in mitochondrial preparations: plasma membranes are removed or selectively permeabilized, while mitochondrial structural and functional integrity is maintained [6]. In mt-preparations, extramitochondrial concentrations of fuel substrates, ADP, ATP, inorganic phosphate (P_i), and cations including H^+ can be controlled to determine mitochondrial respiratory function under a set of conditions defined as coupling control states (Tab. 1). In substrate-uncoupler-inhibitor titration (SUIT) protocols, substrate combinations and specific inhibitors of ET-pathway enzymes are used to obtain defined pathway control states [7,8] (Fig. 1b). Pathway and coupling control states are complementary, since mt-preparations depend on (*1*) an exogenous supply of pathway-specific fuel substrates and O_2, and (*2*) exogenous control of phosphorylation [9].

Reference respiratory states are established with kinetically-saturating substrate concentrations for analysis of mitochondrial respiratory capacities. These delineate — comparable to channel capacity in information theory [10] — the upper boundary of O_2 consumption rates. Intracellular conditions in living cells deviate from these experimental states. Further information is obtained in kinetic studies of flux as a function of fuel substrate concentration, [ADP], or [O_2] in the range between kinetically-saturating concentrations and anoxia [11].

Phosphorylation. The term phosphorylation is used generally in many contexts, *e.g.*, protein phosphorylation. Phosphorylation in the context of OXPHOS is defined as phosphorylation of ADP by P_i to form ATP, coupled to oxidative electron transfer (Fig. 1c,d). The ET- and phosphorylation-pathways comprise coupled components of the OXPHOS-system. P/O is the ratio of P_i to atomic oxygen consumed [9]. The symbol, P», is introduced here as more discriminating and specific than P (Fig. 1c). The symbol P» indicates the endergonic (uphill) direction ADP→ATP, and likewise P« the corresponding exergonic (downhill) hydrolysis ATP→ADP (Fig. 2). $J_{P»}$ and $J_{P«}$ are the corresponding fluxes of ADP phosphorylation and ATP hydrolysis, respectively. P» refers mainly to phosphorylation driven by proton translocation (Fig. 1d),[12] but may also involve substrate-level phosphorylation in the mitochondrial matrix (succinyl-CoA ligase, monofunctional C1-tetrahydrofolate synthase), cytosol (phosphoglycerate kinase and pyruvate kinase), or both (phosphoenolpyruvate carboxykinase isoforms

1 and 2). Kinase cycles are involved in intracellular energy transfer and signal transduction for regulation of energy flux [13].

Respiratory coupling control states: concept and nomenclature

Concept-driven terminology. Respiratory control refers to the ability of mitochondria to adjust O_2 flux in response to external control signals by engaging various mechanisms of control and regulation[14]. Respiratory control is monitored in mt-preparations under conditions defined as respiratory states, preferentially under near-physiological conditions of temperature, pH, and medium ionic composition. When phosphorylation of ADP to ATP is stimulated or depressed, an increase or decrease is observed in electron transfer measured as O_2 flux in respiratory coupling states of intact mitochondria ('controlled states' in the classical terminology of bioenergetics). Alternatively, coupling of electron transfer with phosphorylation is diminished by uncouplers, which eliminates control by P» and increases respiratory rate (noncoupled or 'uncontrolled state'; Tab. 1).

Coupling efficiency is diminished by intrinsic and extrinsic uncoupling. Uncoupling of mitochondrial respiration is a general term comprising diverse mechanisms. Differences of terms — uncoupled *vs.* noncoupled — are easily overlooked, although they relate to different meanings of uncoupling (Tab. 2).

To extend the classical nomenclature on mitochondrial states (State 1 to 5) [15] by a concept-driven terminology that explicitly incorporates information on the meaning of respiratory states, the terminology must be general and not restricted to any particular experimental protocol or mitochondrial preparation [16]. Standard respiratory coupling states are obtained while maintaining a defined ET-pathway state with constant fuel substrates and inhibitors of specific branches of the ET-pathway. The focus of concept-driven nomenclature is primarily the theoretical *why*, along with clarification of the experimental *how* [17].

In the three coupling states **—** LEAK, OXPHOS, and ET **—** the corresponding respiratory rates are abbreviated as *L*, *P*, and *E*, respectively (Fig. 2a). The *pmF* is *maximum* in the LEAK-state of coupled mitochondria, driven by LEAK-respiration at a minimum back-flux of cations to the matrix compartment, *high* in the OXPHOS-state when it drives phosphorylation, and *low* in the ET-state when uncouplers short-circuit the proton cycle (Tab. 1).

LEAK-state - Fig. 2b. The LEAK-state is the state of mitochondrial respiration when O_2 flux mainly compensates for ion leaks in the absence of ATP synthesis, at kinetically-saturating concentrations of O_2 and respiratory fuel substrates. Stimulation of phosphorylation is prevented by (*1*) absence of ADP and ATP; (*2*) maximum ATP/ADP ratio (State 4); or (*3*) inhibition of the phosphorylation-pathway with inhibitors of F_1F_O-ATPase (oligomycin; Omy) or adenine nucleotide translocase (carboxyatractyloside; Tab. 1). The chelator EGTA is added to mt-respiration media to bind free Ca^{2+}, thus limiting cation cycling. LEAK-respiration is the intrinsically uncoupled O_2 consumption without addition of uncouplers. The LEAK-rate is a function of respiratory state, hence it depends on (*1*) the barrier function of the mtIM ('leakiness'), (*2*) the electrochemical potential differences and concentration differences across the mtIM, and (*3*) the H^+/O_2 ratio of the ET-pathway (Fig. 1b).

State 4 is a LEAK-state after depletion of ADP [15]. O_2 flux in State 4 overestimates LEAK-respiration if ATP hydrolysis activity recycles ATP to ADP, $J_{P«}$, which stimulates respiration coupled to phosphorylation, $J_{P»} > 0$. Inhibition of the phosphorylation-pathway by oligomycin ensures that $J_{P»} = 0$ (State 4o; Tab. 1).

OXPHOS-state - Fig. 2c. At any given ET-pathway state, the OXPHOS-state establishes conditions to measure OXPHOS-capacity as a reference, at kinetically-saturating concentrations of O_2, as well as respiratory fuel and phosphorylation substrates. Respiratory OXPHOS-capacities, *P*, are related to ADP-phosphorylation capacities by the ATP yield per O_2 (Fig. 1c).

The OXPHOS-state is compared with State 3, which is the state stimulated by addition of fuel substrates while the ADP concentration in the preceding State 2 (see below) is still 'high' and supports coupled energy transformation in isolated mitochondria in a closed respirometric chamber [15]. Repeated ADP titrations re-establish State 3. Starting at experimental O_2 concentrations, c_{O2}, of air-saturation (193 or 238 µM O_2 at 37 °C or 25 °C and sea level at 1 atm or 101.32 kPa, and an oxygen solubility of respiration medium at 0.92 times that of pure water) [18], the added ADP concentrations must be low

enough (typically 100 to 300 µM) to allow phosphorylation to ATP without O_2 depletion during the transition to State 4. In contrast, kinetically-saturating ADP concentrations are usually 10-fold higher than 'high ADP' (*e.g.*, 2.5 mM) supporting OXPHOS capacity in isolated mitochondria [11].

Electron transfer-state - Fig. 2d. The ET-state is defined as the *noncoupled* state with kinetically-saturating concentrations of O_2 and respiratory substrate, and optimum exogenous uncoupler concentration for maximum O_2 flux (ET-capacity). Uncouplers are weak lipid-soluble acids that function as protonophores. These disrupt the barrier function of the mtIM and thus short-circuit the protonmotive system, functioning like a clutch in a mechanical device. As a consequence of the nearly collapsed *pmF*, the driving force is insufficient for phosphorylation and $J_{P»} = 0$. The most frequently used uncouplers are carbonyl cyanide m-chloro phenyl hydrazone (CCCP), carbonyl cyanide *p*-trifluoromethoxyphenylhydrazone (FCCP), or dinitrophenol (DNP). Stepwise titration of uncouplers stimulates respiration up to or above the level of O_2 consumption rates in the OXPHOS-state; respiration is inhibited, however, above optimum uncoupler concentrations [5].

The abbreviation State 3u is occasionally used to indicate the state of respiration after titration of an uncoupler, without sufficient emphasis on the fundamental difference between OXPHOS-capacity (*well-coupled* with an endogenous uncoupled component) and ET-capacity (*noncoupled*; Fig. 2a).

ROX-state versus anoxia. The state of residual O_2 consumption, ROX, is not a coupling state. The rate of residual oxygen consumption, *Rox*, is defined as O_2 consumption due to oxidative reactions measured after inhibition of ET with antimycin A alone or in combination with rotenone and malonic acid. Cyanide and azide inhibit not only CIV but also catalase and several peroxidases, whereas AOX is not inhibited (Fig. 1b). *Rox* represents a baseline to correct respiration: *Rox*-corrected *L*, *P* and *E* are not only lower than total fluxes, but also change the flux control ratios *L*/*P* and *L*/*E*. *Rox* is not necessarily equivalent to non-mitochondrial respiration, considering O_2-consuming reactions in mitochondria that are not related to ET — such as O_2 consumption in reactions catalyzed by monoamine oxidases, monooxygenases (cytochrome P450 monooxygenases), dioxygenases (trimethyllysine dioxygenase), and several hydoxylases.

In the nomenclature of Chance and Williams, State 2 is induced by titration of ADP before addition of fuel substrates [15,19]. ADP stimulates respiration transiently on the basis of endogenous fuel substrates resulting in phosphorylation of a small portion of the added ADP. State 2 is then a ROX state at minimum respiratory activity after exhaustion of endogenous fuel substrates. State 5 '*may be obtained by antimycin A treatment or by anaerobiosis*' [15]. These definitions give State 5 two different meanings: ROX or anoxia.

Anoxia is induced after exhaustion of O_2 in a closed respirometric chamber. Diffusion of O_2 from the surroundings into the aqueous solution is a confounding factor potentially preventing complete anoxia [11].

Rates and SI units

The term *rate* is not adequately defined to be useful for reporting data. A rate can be (*1*) an extensive quantity [1], termed *flow*, *I*, when expressed per chamber (instrumental system) or per countable, non-divisible *object* (number of cells, organisms, 'in-dividuals'); or (*2*) a size-specific quantity, termed *flux*, *J*, when expressed per volume or mass [2] (Fig. 3).

Different units are used to report the O_2 consumption rate, OCR. SI units provide the common reference with appropriately chosen SI prefixes [1]. Although volume is expressed as m^3 using the SI base unit, the liter [dm^3] is a conventional unit of volume for concentration and is used for most solution chemical kinetics. Constants for conversion to SI units are summarized in Tab. 3.

Normalization of rate per system

Flow: per chamber. The instrumental system (chamber) is part of the measurement instrument, separated from the environment as an isolated, closed, open, isothermal or non-isothermal system. Analyses are restricted to intra-experimental comparison of relative differences, when reporting O_2 flows per respiratory chamber, I_{O_2} [nmol·s^{-1}] (Fig. 3).

Flux: per chamber volume. System volume-specific O_2 flux, J_{V,O_2} (per liquid V of the instrumental chamber [L]), is of methodological interest in relation to the instrumental limit of detection. J_{V,O_2} increases in proportion to sample concentration in the chamber. At an O_2 flow of 100 amol·s^{-1}·cell^{-1} and a cell concentration of 10^9 cells·L^{-1} (10^6 cells·mL^{-1}), J_{V,O_2} is 100 nmol·s^{-1}·L^{-1} (100 pmol·s^{-1}·mL^{-1}). J_{V,O_2} should be independent of the chamber volume at constant sample concentration. There are practical limitations to increasing the sample concentration in the chamber, when one is concerned about crowding effects and instrumental time resolution.

Normalization of rate per sample

Flow: per object. The oxygen flow per countable object, $I_{O_2/\underline{N}X}$, is I_{O_2} divided by the number of objects in the chamber, N_X [x]. The oxygen flow per cell, $I_{O_2/\underline{N}ce}$, is obtained from volume-specific O_2 flux, J_{V,O_2} [nmol·s^{-1}·L^{-1}], divided by the number concentration of cells, $C_{\underline{N}ce}$ [x·L^{-1}]. $C_{\underline{N}ce} = N_{ce}·V^{-1}$, where N_{ce} is the number of cells in the chamber. O_2 flow is expressed in units of attomole (10^{-18} mol) of O_2 consumed per second per cell [amol·s^{-1}·cell^{-1}] [20], numerically equivalent to [pmol·s^{-1}·10^{-6} cells]. Generally, $C_{\underline{N}X}$ is the experimental number concentration of sample X. Several sample types are not countable objects, *e.g.*, tissue homogenate, in which case a sample-specific oxygen flow cannot be expressed.

Size-specific flux: per sample size. Mass-specific flux, $J_{O_2/\underline{m}X}$ [mol·s^{-1}·kg^{-1}], expresses respiration normalized per mass of the sample. Mass-specific oxygen flux integrates the quality and density of mitochondria, and thus provides the appropriate normalization for evaluation of tissue performance. When studying isolated mitochondria and homogenized or permeablized tissues and cells, $J_{O_2/\underline{m}X}$ should be independent of the mass-concentration of the subsample obtained from the same tissue or cell culture. $I_{O_2/\underline{N}ce}$ can be directly compared only between cells of identical size. To take into account differences in cell size, normalization is required to obtain cell size-specific flux, $J_{O_2/\underline{m}ce}$ or $J_{O_2/\underline{V}ce}$ [21] (Fig. 3).

Marker-specific flux: per mitochondrial content. To evaluate differences in mitochondrial respiration independent of mitochondrial density, flux is normalized for structural or functional mt-elementary markers, *mtE*, expressed in marker-specific mt-elementary units [mtEU] (Fig. 3). For example, citrate synthase (CS) activity is a frequently applied functional *mtE* expressed in international units, IU [µmol·min^{-1}] (1 IU of CS forms 1 µmol of citrate per min; although the SI unit [nmol·s^{-1}] would be preferable). Then the mtEU is taken as [µmol·min^{-1}] or [nmol·s^{-1}]. Volume-specific oxygen flux, J_{V,O_2} [pmol·s^{-1}·mL^{-1}], is divided by CS activity expressed per chamber volume [mtEU·mL^{-1}], to obtain marker-specific respiratory flux, $J_{O_2/mtE}$ [pmol·s^{-1}·mtEU^{-1}]. Alternatively, $J_{O_2/mtE}$ is calculated from tissue mass-specific flux of permeabilized muscle fibers, $J_{O_2/\underline{m}}$ [pmol O_2·s^{-1}·mg^{-1}], divided by tissue mass-specific CS activity [mtEU·mg^{-1}]. $J_{O_2/mtE}$ is independent of mitochondrial density. If the respirometric and enzymatic assays are performed at an identical temperature, OXPHOS- or ET-capacity can be compared with the capacity of CS as a regulatory enzyme in the tricarboxylic acid (TCA) cycle, which is of interest in the context of metabolic flux control.

One cannot assume that quantitative changes in various markers — such as CS activity, other mitochondrial enzyme activities or protein content — necessarily occur in parallel with one another [22]. It should be established that the marker chosen is not selectively altered by the compared trait or treatment. In conclusion, the normalization must reflect the question under investigation. On the other hand, the goal of combining results across projects and institutions requires standardization of normalization for entry into a databank.

Comparable to the concept of the respiratory acceptor control ratio, *RCR* = State 3/State 4,[9] the most readily applied normalization is that of flux control ratios and flux control factors [8,16]. Then, instead of a specific mt-enzyme activity, the respiratory activity in a reference state serves as the *mtE*, yielding a dimensionless ratio of two fluxes measured consecutively in the same respirometric titration protocol. Selection of the state of maximum flux in a protocol as the reference state — *e.g.*, ET-state in *L*/*E* and *P*/*E* flux control ratios [16] — has the advantages of: (*1*) elimination of experimental variability in additional measurements, such as determination of enzyme activity or tissue mass; (*2*) statistically validated linearization of the response in the range of 0 to 1; and (*3*) consideration of maximum flux for integrating a large number of metabolic steps in the OXPHOS- or ET-pathways. This reduces the risk

of selecting a functional marker that is specifically altered by the treatment or pathology, yet increases the chance that the highly integrative pathway is affected, *e.g.*, the OXPHOS- rather than ET-pathway in case of an enzymatic defect in the phosphorylation-pathway. In this case, additional information can be obtained by reporting flux control ratios based on a reference state that indicates stable tissue mass-specific flux.

Conclusions

Clarity of concepts on mitochondrial respiratory control can serve as a gateway to better diagnose mitochondrial respiratory adaptations and defects linked to genetic variation, age-related health risks, sex-specific mitochondrial performance, lifestyle with its effects on degenerative diseases, and thermal and chemical environment. The challenges of measuring mitochondrial respiratory flux are matched by those of normalization: We distinguish between (*1*) the instrumental *system* or *chamber* with volume V and mass m defined by the system boundaries, and (*2*) the *sample* or *objects* with volume V_X and mass m_X that are enclosed in the instrumental chamber. Metabolic O_2 *flow* per countable object increases as the size of the object is increased. This confounding factor is eliminated by expressing respiration as mass-specific or cell volume-specific O_2 *flux*. The present recommendations on coupling control states and respiratory rates are focused on studies using mitochondrial preparations. Terms and symbols are summarized in Tab. 4. These need to be complemented by considerations on pathway control of mitochondrial respiration [7,8,23], respiratory states and rates in living cells, respiratory flux control ratios, and harmonization of experimental procedures. The present perspective is extended in a more detailed overview on quantitiative mitochondrial physiology [24].

References

1. Cohen, E. R. et al. *IUPAC Green Book, 3rd Edition, 2nd Printing, IUPAC & RSC Publishing, Cambridge* (2008).
2. Gnaiger, E. *Pure Appl Chem* **65**, 1983-2002 (1993).
3. Beard, D. A. *PLoS Comput Biol* **1**, e36 (2005).
4. Mitchell, P. *Nature* **191**, 144-148 (1961).
5. Mitchell, P. *Biochim Biophys Acta Bioenergetics* **1807**, 1507-1538 (2011).
6. Schmitt, S. et al. *Anal Biochem* **443**, 66-74 (2013).
7. Doerrier, C. et al. *Methods Mol Biol* **1782**, 31-70 (2018).
8. §Gnaiger, E. *Bioenerg Commun* **2020.2**, doi:10.26124/bec:2020-0002.v1 (2020).
9. Chance, B. & Williams, G. R. *J Biol Chem* **217**, 383-393 (1955).
10. Schneider, T. D. *IEEE Eng Med Biol Mag* **25**, 30-33 (2006).
11. Gnaiger, E. *Respir Physiol* **128**, 277-297 (2001).
12. Watt, I. N. et al. *Proc Natl Acad Sci U S A* **107**, 16823-16827 (2010).
13. Németh, B. et al. *FASEB J* **30**, 286-300 (2016).
14. Fell, D. *Understanding the control of metabolism. Portland Press* (1997).
15. Chance, B. & Williams, G. R. *J Biol Chem* **217**, 409-427 (1955).
16. Gnaiger, E. *Int J Biochem Cell Biol* **41**, 1837-1845 (2009).
17. Miller, G. A. *The science of words. Scientific American Library New York* (1991).
18. Forstner, H. & Gnaiger, E. *In: Polarographic Oxygen Sensors. Aquatic and Physiological Applications. Gnaiger, E. & Forstner, H. (eds), Springer, Berlin, Heidelberg, New York*, 321-333 (1983).
19. Chance, B. & Williams, G. R. *Adv Enzymol Relat Subj Biochem* **17**, 65-134 (1956).
20. Wagner, B. A., Venkataraman, S. & Buettner, G. R. *Free Radic Biol Med* **51**, 700-712 (2011).
21. Renner, K. et al. *Biochim Biophys Acta* **1642**, 115-123 (2003).
22. Drahota, Z. et al. *Physiol Res* **53**, 119-122 (2004).
23. Schöpf, B. et al. *Nat Commun* **11**, 1487 (2020).
24. §Gnaiger, E. et al. *Bioenerg Commun* **2020.1**, doi:10.26124/bec:2020-0001.v1 (2020).
25. Canton, M. et al. *Biochem J* **310**, 477-481 (1995).
26. Rich, P. R. *Encyclopedia Biol Chem* **1**, 467-472 (2013).
27. Lemieux, H., Blier, P. U. & Gnaiger, E. *Sci Rep* **7**, 2840 (2017).

§ To be released with DOI until acceptance by *Nat Metab*

At present:

8. Gnaiger, E. *Mitochondr Physiol Network 19.12. Oroboros MiPNet Publications, Innsbruck* (2014).
24. Gnaiger, E. et al. *MitoFit Preprint Arch* doi:10.26124/mitofit:190001.v6 (2019).

***Authors (MitoEAGLE Task Group):** Gnaiger Erich, Aasander Frostner Eleonor, Abdul Karim Norwahidah, Abdel-Rahman Engy Ali, Abumrad Nada A, Acuna-Castroviejo Dario, Adiele Reginald C, Ahn Bumsoo, Alencar Mayke Bezerra, Ali Sameh S, Almeida Angeles, Alton Lesley, Alves Marco G, Amati Francesca, Amoedo Nivea Dias, Amorim Ricardo, Anderson Ethan J, Andreadou Ioanna, Antunes Diana, Arago Marc, Aral Cenk, Arandarcikaite Odeta, Arias-Reyes Christian, Armand Anne-Sophie, Arnould Thierry, Avram Vlad F, Axelrod Christopher L, Bailey Damian M, Bairam Aida, Bajpeyi Sudip, Bajzikova Martina, Bakker Barbara M, Banni Aml, Bardal Tora, Barlow J, Bastos Sant'Anna Silva Ana Carolina, Batterson Philip M, Battino Maurizio, Bazil Jason N, Beard Daniel A, Bednarczyk Piotr, Beleza Jorge, Bello Fiona, Ben-Shachar Dorit, Bento Guida Jose Freitas, Bergdahl Andreas, Berge Rolf K, Bergmeister Lisa, Bernardi Paolo, Berridge Michael V, Bettinazzi Stefano, Bishop David J, Blier Pierre U, Blindheim Dan Filip, Boardman Neoma T, Boetker Hans Erik, Borchard Sabine, Boros Mihaly, Boersheim Elisabet, Borras Consuelo, Borutaite Vilma, Botella Javier, Bouillaud Frederic, Bouitbir Jamal, Boushel Robert C, Bovard Josh, Bravo-Sagua Roberto, Breton Sophie, Brown David A, Brown Guy C, Brown Robert Andrew, Brozinick Joseph T, Buettner Garry R, Burtscher Johannes, Bustos Matilde, Calabria Elisa, Calbet Jose AL, Calzia Enrico, Cannon Daniel T, Cano Sanchez Maria Consolacion, Canto Alvarez Carles, Cardinale Daniele A, Cardoso Luiza HD, Carvalho Eugenia, Casado Pinna Marta, Cassar Samantha, Castelo Rueda Maria Paulina, Castilho Roger F, Cavalcanti-de-Albuquerque Joao Paulo, Cecatto Cristiane, Celen Murat C, Cervinkova Zuzana, Chabi Beatrice, Chakrabarti Lisa, Chakrabarti Sasanka, Chaurasia Bhagirath, Chen Quan, Chicco Adam J, Chinopoulos Christos, Chowdhury Subir Kumar, Cizmarova Beata, Clementi Emilio, Coen Paul M, Cohen Bruce H, Coker Robert H, Collin-Chenot Anne, Coughlan Melinda T, Coxito Pedro, Crisostomo Luis, Crispim Marcell, Crossland Hannah, Dahdah Norma Ramon, Dalgaard Louise T, Dambrova Maija, Danhelovska Tereza, Darveau Charles-A, Darwin Paula M, Das Anibh Martin, Dash Ranjan K, Davidova Eliska, Davis Michael S, Dayanidhi Sudarshan, De Bem Andreza Fabro, De Goede Paul, De Palma Clara, De Pinto Vito, Dela Flemming, Dembinska-Kiec Aldona, Detraux Damian, Devaux Yvan, Di Marcello Marco, Di Paola Floriana Jessica, Dias Candida, Dias Tania R, Diederich Marc, Distefano Giovanna, Djafarzadeh Siamak, Doermann Niklas, Doerrier Carolina, Dong Lan-Feng, Donnelly Chris, Drahota Zdenek, Duarte Filipe Valente, Dubouchaud Herve, Duchen Michael R, Dumas Jean-Francois, Durham William J, Dymkowska Dorota, Dyrstad Sissel E, Dyson Alex, Dzialowski Edward M, Eaton Simon, Ehinger Johannes K, Elmer Eskil, Endlicher Rene, Engin Ayse Basak, Escames Germaine, Evinova Andrea, Ezrova Zuzana, Falk Marni J, Fell David A, Ferdinandy Peter, Ferko Miroslav, Fernandez-Vizarra Erika, Ferreira Julio Cesar B, Ferreira Rita Maria P, Ferri Alessandra, Fessel Joshua Patrick, Festuccia William T, Filipovska Aleksandra, Fisar Zdenek, Fischer Christine, Fischer Michael J, Fisher Gordon, Fisher Joshua J, Fontanesi Flavia, Ford Ellen, Fornaro Mara, Fuertes Agudo Marina, Fulton Montana, Galina Antonio, Galkin Alexander, Gallee Leon, Galli Gina L J, Gama Perez Pau, Gan Zhenji, Ganetzky Rebecca, Gao Yun, Garcia Geovana S, Garcia-Rivas Gerardo, Garcia-Roves Pablo Miguel, Garcia-Souza Luiz F, Garlid Keith D, Garrabou Gloria, Garten Antje, Gastaldelli Amalia, Gayen Jiaur, Genders Amanda J, Genova Maria Luisa, Giampieri Francesca, Giovarelli Matteo, Glatz Jan FC, Goikoetxea Usandizaga Naroa, Goncalo Teixeira da Silva Rui, Goncalves Debora Farina, Gonzalez-Armenta Jenny L, Gonzalez-Franquesa Alba, Gonzalez-Freire Marta, Gonzalo Hugo, Goodpaster Bret H, Gorr Thomas A, Gourlay Campbell W, Grams Bente, Granata Cesare, Grefte Sander, Grilo Luis, Guarch Meritxell Espino, Gueguen Naig, Gumeni Sentiljana, Haas Clarissa, Haavik Jan, Hachmo Yafit, Haendeler Judith, Haider Markus, Hajrulahovic Anesa, Hamann Andrea, Han Jin, Han Woo Hyun, Hancock Chad R, Hand Steven C, Handl Jiri, Hansikova Hana, Hardee Justin P, Hargreaves Iain P, Harper Mary-Ellen, Harrison David K, Hassan Hazirah, Hatokova Zuzana, Hausenloy Derek J, Heales Simon JR, Hecker Matthias, Heiestad Christina, Hellgren Kim T, Henrique Alexandrino, Hepple Russell T, Hernansanz-Agustin Pablo, Hewakapuge Sudinna, Hickey Anthony J, Ho Dieu Hien, Hoehn Kyle L, Hoel Fredrik, Holland Olivia J, Holloway Graham P, Holzner Lorenz, Hoppel Charles L, Hoppel Florian, Hoppeler Hans, Houstek Josef, Huete-Ortega Maria, Hyrossova Petra, Iglesias-Gonzalez Javier, Irving Brian A, Isola Raffaella, Iyer Shilpa, Jackson Christopher Benjamin, Jadiya Pooja, Jana Prado Fabian, Jandeleit-Dahm Karin, Jang David H, Jang Young Charles, Janowska Joanna, Jansen Kirsten M, Jansen-Duerr Pidder, Jansone Baiba, Jarmuszkiewicz Wieslawa, Jaskiewicz Anna, Jaspers Richard T, Jedlicka Jan, Jerome Estaquier, Jespersen Nichlas Riise, Jha Rajan Kumar, Jones John G, Joseph Vincent, Jurczak Michael J, Jurk Diana, Jusic Amela, Kaambre Tuuli, Kaczor Jan Jacek, Kainulainen Heikki, Kampa Rafal Pawel, Kandel Sunil Mani, Kane Daniel A,

Kapferer Werner, Kapnick Senta, Kappler Lisa, Karabatsiakis Alexander, Karavaeva Iuliia, Karkucinska-Wieckowska Agnieszka, Kaur Sarbjot, Keijer Jaap, Keller Markus A, Keppner Gloria, Khamoui Andy V, Kidere Dita, Kilbaugh Todd, Kim Hyoung Kyu, Kim Julian KS, Kimoloi Sammy, Klepinin Aleksandr, Klepinina Lyudmila, Klingenspor Martin, Klocker Helmut, Kolassa Iris, Komlodi Timea, Koopman Werner JH, Kopitar-Jerala Natasa, Kowaltowski Alicia J, Kozlov Andrey V, Krajcova Adela, Krako Jakovljevic Nina, Kristal Bruce S, Krycer James R, Kuang Jujiao, Kucera Otto, Kuka Janis, Kwak Hyo Bum, Kwast Kurt E, Kwon Oh Sung, Laasmaa Martin, Labieniec-Watala Magdalena, Lagarrigue Sylviane, Lai Nicola, Lalic Nebojsa M, Land John M, Lane Nick, Laner Verena, Lanza Ian R, Laouafa Sofien, Laranjinha Joao, Larsen Steen, Larsen Terje S, Lavery Gareth G, Lazou Antigone, Ledo Ana Margarida, Lee Hong Kyu, Leeuwenburgh Christiaan, Lehti Maarit, Lemieux Helene, Lenaz Giorgio, Lerfall Joergen, Li Pingan Andy, Li Puma Lance, Liang Liping, Liepins Edgars, Lin Chien-Te, Liu Jiankang, Lopez Garcia Luis Carlos, Lucchinetti Eliana, Ma Tao, Macedo Maria Paula, Machado Ivo F, Maciej Sarah, MacMillan-Crow Lee Ann, Magalhaes Jose, Magri Andrea, Majtnerova Pavlina, Makarova Elina, Makrecka-Kuka Marina, Malik Afshan N, Marcouiller Francois, Markova Michaela, Markovic Ivanka, Martin Daniel S, Martins Ana Dias, Martins Joao D, Maseko Tumisang Edward, Maull Felicia, Mazat Jean-Pierre, McKenna Helen T, McKenzie Matthew, McMillan Duncan GG, Mendham Amy, Menze Michael A, Mercer John R, Merz Tamara, Messina Angelina, Meszaros Andras, Methner Axel, Michalak Slawomir, Mila Guasch Maria, Minuzzi Luciele M, Moellering Douglas R, Moisoi Nicoleta, Molina Anthony JA, Montaigne David, Moore Anthony L, Moore Christy, Moreau Kerrie, Moreira Bruno P, Moreno-Sanchez Rafael, Mracek Tomas, Muccini Anna Maria, Munro Daniel, Muntane Jordi, Muntean Danina M, Murray Andrew James, Musiol Eva, Nabben Miranda, Nair K Sreekumaran, Nehlin Jan O, Nemec Michal, Nesci Salvatore, Neufer P Darrell, Neuzil Jiri, Neviere Remi, Newsom Sean A, Norman Jennifer, Nozickova Katerina, Nunes Sara, O'Brien Kristin, O'Brien Katie A, O'Gorman Donal, Olgar Yusuf, Oliveira Ben, Oliveira Jorge, Oliveira Marcus F, Oliveira Marcos Tulio, Oliveira Pedro Fontes, Oliveira Paulo J, Olsen Rolf Erik, Orynbayeva Zulfiya, Osiewacz Heinz D, Paez Hector, Pak Youngmi Kim, Pallotta Maria Luigia, Palmeira Carlos, Parajuli Nirmala, Passos Joao F, Passrugger Manuela, Patel Hemal H, Pavlova Nadia, Pavlovic Kasja, Pecina Petr, Pedersen Tina M, Perales Jose Carles, Pereira da Silva Grilo da Silva Filomena, Pereira Rita, Pereira Susana P, Perez Valencia Juan Alberto, Perks Kara L, Pesta Dominik, Petit Patrice X, Pettersen Nitschke Ina Katrine, Pichaud Nicolas, Pichler Irene, Piel Sarah, Pietka Terri A, Pinho Sonia A, Pino Maria F, Pirkmajer Sergej, Place Nicolas, Plangger Mario, Porter Craig, Porter Richard K, Preguica Ines, Prigione Alessandro, Procaccio Vincent, Prochownik Edward V, Prola Alexandre, Pulinilkunnil Thomas, Puskarich Michael A, Puurand Marju, Radenkovic Filip, Ramzan Rabia, Rattan Suresh IS, Reano Simone, Reboredo-Rodriguez Patricia, Rees Bernard B, Renner-Sattler Kathrin, Rial Eduardo, Robinson Matthew M, Roden Michael, Rodrigues Ana Sofia, Rodriguez Enrique, Rodriguez-Enriquez Sara, Roesland Gro Vatne, Rohlena Jakub, Rolo Anabela Pinto, Ropelle Eduardo R, Roshanravan Baback, Rossignol Rodrigue, Rossiter Harry B, Rousar Tomas, Rubelj Ivica, Rybacka-Mossakowska Joanna, Saada Reisch Ann, Safaei Zahra, Salin Karine, Salvadego Desy, Sandi Carmen, Saner Nicholas, Santos Diana, Sanz Alberto, Sardao Vilma, Sarlak Saharnaz, Sazanov Leonid A, Scaife Paula, Scatena Roberto, Schartner Melanie, Scheibye-Knudsen Morten, Schilling Jan M, Schlattner Uwe, Schmitt Sabine, Schneider Gasser Edith Mariane, Schoenfeld Peter, Schots Pauke C, Schulz Rainer, Schwarzer Christoph, Scott Graham R, Selman Colin, Sendon Pamella Marie, Shabalina Irina G, Sharma Pushpa, Sharma Vipin, Shevchuk Igor, Shirazi Reza, Shiroma Jonathan G, Siewiera Karolina, Silber Ariel M, Silva Ana Maria, Sims Carrie A, Singer Dominique, Singh Brijesh Kumar, Skolik Robert A, Smenes Benedikte Therese, Smith James, Soares Felix Alexandre Antunes, Sobotka Ondrej, Sokolova Inna, Solesio Maria E, Soliz Jorge, Sommer Natascha, Sonkar Vijay K, Sova Marina, Sowton Alice P, Sparagna Genevieve C, Sparks Lauren M, Spinazzi Marco, Stankova Pavla, Starr Jonathan, Stary Creed, Stefan Eduard, Stelfa Gundega, Stepto Nigel K, Stevanovic Jelena, Stiban Johnny, Stier Antoine, Stocker Roland, Storder Julie, Sumbalova Zuzana, Suomalainen Anu, Suravajhala Prashanth, Svalbe Baiba, Swerdlow Russell H, Swiniuch Daria, Szabo Ildiko, Szewczyk Adam, Szibor Marten, Tanaka Masashi, Tandler Bernard, Tarnopolsky Mark A, Tausan Daniel, Tavernarakis Nektarios, Teodoro Joao Soeiro, Tepp Kersti, Thakkar Himani, Thapa Maheshwor, Thyfault John P, Tomar Dhanendra, Ton Riccardo, Torp May-Kristin, Torres-Quesada Omar, Towheed Atif, Treberg Jason R, Tretter Laszlo, Trewin Adam J, Trifunovic Aleksandra, Trivigno Catherine, Tronstad Karl Johan, Trougakos Ioannis P, Truu Laura, Tuncay Erkan, Turan Belma, Tyrrell Daniel J, Urban Tomas, Urner Sofia, Valentine Joseph Marco, Van Bergen Nicole J, Van der Ende Miranda, Varricchio Frederick, Vaupel Peter, Vella

Joanna, Vendelin Marko, Vercesi Anibal E, Verdaguer Ignasi Bofill, Vernerova Andrea, Victor Victor Manuel, Vieira Ligo Teixeira Camila, Vidimce Josif, Viel Christian, Vieyra Adalberto, Vilks Karlis, Villena Josep A, Vincent Vinnyfred, Vinogradov Andrey D, Viscomi Carlo, Vitorino Rui Miguel Pinheiro, Vlachaki Walker Julia, Vogt Sebastian, Volani Chiara, Volska Kristine, Votion Dominique-Marie, Vujacic-Mirski Ksenija, Wagner Brett A, Ward Marie Louise, Warnsmann Verena, Wasserman David H, Watala Cezary, Wei Yau-Huei, Weinberger Klaus M, Weissig Volkmar, White Sarah Haverty, Whitfield Jamie, Wickert Anika, Wieckowski Mariusz R, Wiesner Rudolf J, Williams Caroline M, Winwood-Smith Hugh, Wohlgemuth Stephanie E, Wohlwend Martin, Wolff Jonci Nikolai, Wrutniak-Cabello Chantal, Wuest Rob CI, Yokota Takashi, Zablocki Krzysztof, Zanon Alessandra, Zanou Nadege, Zaugg Kathrin, Zaugg Michael, Zdrazilova Lucie, Zhang Yong, Zhang Yizhu, Zikova Alena, Zischka Hans, Zorzano Antonio, Zujovic Tijana, Zvejniece Liga

Affiliations:

https://www.bioenergetics-communications.org/index.php/BEC2020.1_doi10.26124bec2020-0001.v1

Acknowledgements

We thank Beno M for management assistance, and Rich PR for valuable discussions. This publication is based upon work from COST Action CA15203 MitoEAGLE, supported by COST (European Cooperation in Science and Technology), in cooperation with COST Actions CA16225 EU-CARDIOPROTECTION and CA17129 CardioRNA, and K-Regio project MitoFit funded by the Tyrolian Government.

Author contributions

This manuscript developed as an open invitation to scientists and students to join as coauthors in the bottom-up spirit of COST, based on a first draft written by the corresponding author, who integrated coauthor contributions in a sequence of Open Access versions. Coauthors contributed to the scope and quality of the manuscript, may have focused on a particular section, and are listed in alphabetical order. Coauthors confirm that they have read the final manuscript and agree to implement the recommendations into future manuscripts, presentations and teaching materials.

Competing interests

E.G. is founder and CEO of Oroboros Instruments, Innsbruck, Austria. The other authors declare no competing financial interests.

Tables

Table 1 | Coupling control states and rates, and residual oxygen consumption in mitochondrial preparations. Respiration- and phosphorylation-flux, J_{kO_2} and $J_{P»}$, are rates, characteristic of a state in conjunction with the protonmotive force, *pmF*. Coupling states are established at kinetically-saturating concentrations of fuel substrates and O_2.

State	Rate	J_{kO_2}	$J_{P»}$	*pmF*	Inducing factors	Limiting factors
LEAK	*L*	low, cation leak-dependent respiration	0	max.	back-flux of cations including proton leak, proton slip	$J_{P»}$ = 0: (*1*) without ADP, *L*(n); (*2*) max. ATP/ADP ratio, *L*(T); or (*3*) inhibition of the phosphorylation-pathway, *L*(Omy)
OXPHOS	*P*	high, ADP-stimulated respiration, OXPHOS-capacity	max.	high	kinetically-saturating [ADP] and [P_i]	$J_{P»}$ by phosphorylation-pathway capacity; or J_{kO_2} by ET-capacity
ET	*E*	max., noncoupled respiration, ET-capacity	0	low	optimal external uncoupler concentration for max. $J_{O_2,E}$	J_{kO_2} by ET-capacity
ROX	*Rox*	min., residual O_2 consumption	0	0	$J_{O_2,Rox}$ in non-ET-pathway oxidation reactions	inhibition of all ET-pathways; or absence of fuel substrates

488 **Table 2 | Terms on respiratory coupling and uncoupling**
489

	Term	J_{kO_2}	P»/O_2	Notes
intrinsic, no protonophore added	uncoupled	*L*	0	non-phosphorylating LEAK-respiration (Fig. 2)
	proton leak-uncoupled		0	component of *L*, H^+ diffusion across the mtIM (Fig. 2b-d)
	inducibly uncoupled		0	by UCP1 or cation (*e.g.*, Ca^{2+}) cycling; strongly stimulated by permeability transition (mtPT); experimentally induced by valinomycin in the presence of K^+
	decoupled		0	component of *L*, proton slip when protons are effectively not pumped in the redox proton pumps CI, CIII and CIV or are not driving phosphorylation (F-ATPase) [25] (Fig. 2b-d)
	loosely coupled		0	component of *L*, lower coupling due to superoxide formation and bypass of proton pumps by electron leak with univalent reduction of O_2 to superoxide ($O2^{\bullet-}$; superoxide anion radical)
	dyscoupled		0	mitochondrial dysfunction due to pathologically, toxicologically, environmentally increased uncoupling
noncoupled		*E*	0	ET-capacity, non-phosphorylating respiration stimulated to maximum flux at optimum exogenous protonophore concentration (Fig. 2d)
well-coupled		*P*	high	OXPHOS-capacity, phosphorylating respiration with an intrinsic LEAK component (Fig. 2c)
fully coupled		*P – L*	max.	OXPHOS-capacity corrected for LEAK-respiration (Fig. 2a)
acoupled			0	electron transfer in mitochondrial fragments without vectorial proton translocation upon loss of vesicular (compartmental) integrity

490
491

Table 3 | Conversion of units

a. Conversion of O_2 flow, I_{O_2}, to SI units (e^- is the number of electrons or reducing equivalents)

1 Unit	·	Multiplication factor	SI-unit
ng.atom O·s^{-1}	(2 e$^-$)	0.5	nmol O_2·s^{-1}
ng.atom O·min^{-1}	(2 e$^-$)	8.33	pmol O_2·s^{-1}
natom O·min^{-1}	(2 e$^-$)	8.33	pmol O_2·s^{-1}
nmol O_2·min^{-1}	(4 e$^-$)	16.67	pmol O_2·s^{-1}
nmol O_2·h^{-1}	(4 e$^-$)	0.2778	pmol O_2·s^{-1}

b. Conversion of units with preservation of numerical values

Name	Frequently used unit	Equivalent unit	Notes
volume-specific flux, J_{V,O_2}	pmol·s^{-1}·mL^{-1}	nmol·s^{-1}·L^{-1}	1
	mmol·s^{-1}·L^{-1}	mol·s^{-1}·m^{-3}	
cell-specific flow, $I_{O_2/\underline{N}ce}$	pmol·s^{-1}·10^{-6} cells	amol·s^{-1}·cell^{-1}	2
	pmol·s^{-1}·10^{-9} cells	zmol·s^{-1}·cell^{-1}	3
cell number concentration, $C_{\underline{N}ce}$	10^6 cells·mL^{-1}	10^9 cells·L^{-1}	
mitochondrial protein concentration, C_{mtE}	0.1 mg·mL^{-1}	0.1 g·L^{-1}	
mass-specific flux, $J_{O_2/\underline{m}}$	pmol·s^{-1}·mg^{-1}	nmol·s^{-1}·g^{-1}	4
volume	1,000 L	m^3 (1,000 kg)	
	L	dm^3 (kg)	
	mL	cm^3 (g)	
	µL	mm^3 (mg)	
	fL	µm^3 (pg)	5
amount of substance concentration	M = mol·L^{-1}	mol·dm^{-3}	

1 pmol: picomole = 10^{-12} mol
2 amol: attomole = 10^{-18} mol
3 zmol: zeptomole = 10^{-21} mol
4 nmol: nanomole = 10^{-9} mol
5 fL: femtolitre = 10^{-15} L

Table 4 | Terms, symbols, and units. SI base units are used, except for the liter [L = dm^3]

Term	Symbol	Unit	Links and comments
alternative quinol oxidase	AOX		Fig. 1b
adenosine diphosphate	ADP		Tab. 1; Fig. 1 and 2
adenosine triphosphate	ATP		Tab. 1; Fig. 1 and 2
ATP hydrolysis ATP→ADP	P«		Fig. 2b,c
catabolic reaction	k		Tab. 1 and 2; Fig. 1 and 2
catabolic respiration	J_{kO_2}	*varies*	Fig 1c, Fig. 2b-d
cell concentration (number [x])	$C_{\underline{N}ce}$	[x·L^{-1}]	for normalization of rate
coenzyme Q-junction	Q-junction		Fig. 1b
electron transfer Complexes	CI to CIV		Fig. 1b; F_1F_O-ATPase is not an ET- but a phosphorylation-pathway Complex, hence the term Complex V should not be used
electron transfer, state	ET		Tab. 1; Fig. 2a (State 3u)
electron transfer system	ETS		Fig. 1b
ET-capacity	*E*	*varies*	Tab. 1; Fig. 2a,d; rate
ET-excess capacity	*E-P*	*varies*	Fig. 2a
flow	*I*	[mol·s^{-1}]	Fig. 3; extensive quantity
flux	*J*	*varies*	Fig. 3; size-specific quantitiy
inorganic phosphate	P_i		Fig. 1d
inorganic phosphate carrier	PiC		Fig. 1d
LEAK-state	LEAK		Tab. 1; Fig. 2a (compare State 4)
LEAK-respiration	*L*	*varies*	rate; Tab. 1; Fig. 2a,b
mass of sample or objext *X*	m_X or $m_{\underline{N}X}$	[kg] or [kg·x^{-1}]	Fig. 3
mass, dry mass	m_d	[kg] or [kg·x^{-1}]	(dry weight)
mass, wet mass	m_w	[kg] or [kg·x^{-1}]	(wet weight)
mitochondria or mitochondrial	mt		compare mtDNA
mitochondrial elementary marker	*mtE*	[mtEU]	Fig. 3; quantity of mt-marker
mitochondrial elementary unit	mtEU	*varies*	Fig. 3; specific units for mt-marker
mitochondrial inner membrane	mtIM		Fig. 1 (MIM)
mitochondrial outer membrane	mtOM		Fig. 1 (MOM)
NADH-junction	N-junction		Fig. 1b
number concentration of *X*	$C_{\underline{N}X}$	[x·L^{-1}]	for normalization of rate
number format	$\underline{N}$	[x]	Fig. 3
number of cells	N_{ce}	[x]	for normalization of rate
number of entities *X*	N_X	[x]	Fig. 3; for normalization of rate
O_2 concentration	$c_{O_2} = n_{O_2} \cdot V^{-1}$	[mol·L^{-1}]	[O_2]
O_2 flow per countable object	$I_{O_2/\underline{N}X}$	[mol·s^{-1}·x^{-1}]	Fig. 3
O_2 flow per chamber	I_{O_2}	[mol·s^{-1}]	Fig. 3
O_2 flux, in reaction r	J_{rO_2}	*varies*	Fig. 1a
O_2 flux, volume-specific	J_{V,O_2}	[mol·s^{-1}·L^{-1}]	Fig. 3; per volume of chamber
O_2 flux, sample mass-specific	$J_{O_2/\underline{m}X}$	[mol·s^{-1}·kg^{-1}]	Fig. 3; specify dry or wet mass
oxidative phosphorylation	OXPHOS		Fig. 1
OXPHOS-state	OXPHOS		Tab. 1; Fig. 2a (State 3 at kinetically-saturating [ADP] and [P_i])
OXPHOS-capacity	*P*	*varies*	rate; Tab. 1; Fig. 2a,c
permeability transition	mtPT		Tab. 2; MPT is widely used
phosphorylation flux ADP→ATP	$J_{P»}$	*varies*	Fig. 2b-d
phosphorylation of ADP to ATP	P»		Fig. 1
P»/O_2 ratio	P»/O_2		mechanistic $Y_{P»/O_2}$, calculated from pump stoichiometries; Fig. 1c

proton in the negative compartment	H^+_{neg}		Fig. 2b-d
proton in the positive compartment	H^+_{pos}		Fig. 1b,c; Fig. 2b-d
protonmotive flux to the negative compartment	J_{mH^+neg}	*varies*	Fig. 2d,f
protonmotive flux to the positive compartment	J_{mH^+pos}	*varies*	Fig. 2b,c,d
protonmotive force	*pmF*	[V]	Figures 1, 2A and 4; Table 1
rate of electron transfer in ET-state	*E*	*varies*	Tab. 1; ET-capacity
rate of LEAK-respiration	*L*	*varies*	Tab. 1; *L*(n), *L*(T), *L*(Omy)
rate of oxidative phosphorylation	*P*	*varies*	Tab. 1; OXPHOS-capacity
rate of residual oxygen consumption	*Rox*	*varies*	Tab. 1
residual oxygen consumption, state	ROX		Tab. 1
sample type	*X*		
substrate-uncoupler-inhibitor-titration protocol	SUIT		
tricarboxylic acid cycle	TCA cycle		Fig. 1a
volume	*V*	[L]	
volume format	$\underline{V}$	[L]	Fig. 3
volume of sample or object *X*	V_X or $V_{\underline{N}X}$	[L] or [L·x^{-1}]	Fig. 3

Figures

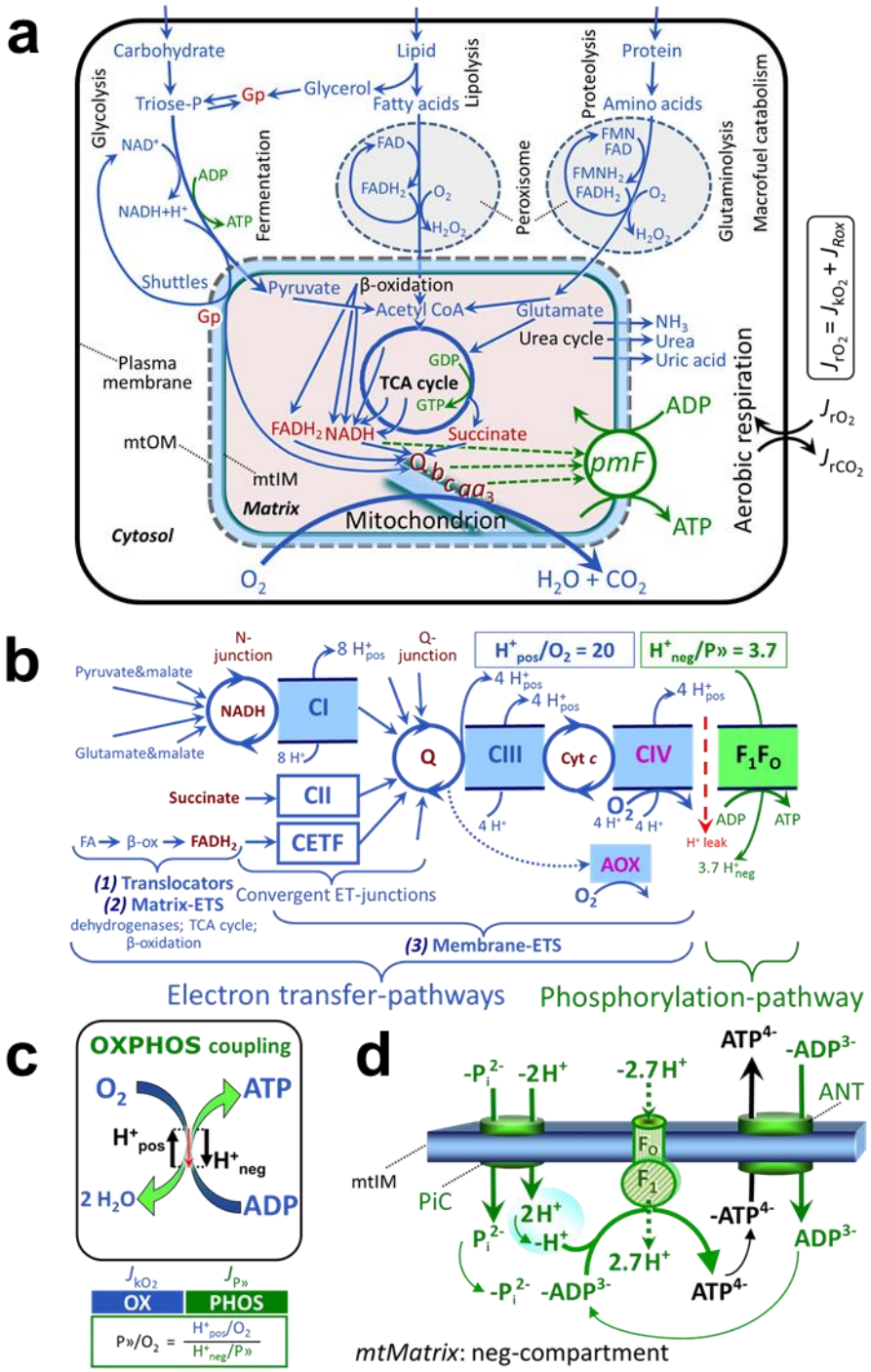

Fig. 1. | Respiration and oxidative phosphorylation (OXPHOS). (a) Cell respiration: uptake of small molecules and catabolism of macronutrients provide the mitochondrial fuel substrates (electron donors), which are oxidized with electron transfer to O_2 (electron acceptor). Dashed arrows indicate the connection between the redox proton pumps (respiratory Complexes CI, CIII and CIV) and the transmembrane protonmotive force, *pmF*. Coenzyme Q (Q) and the cytochromes *b*, *c*, and aa_3 are redox systems of the mitochondrial inner membrane, mtIM. Glycerol-3-phosphate, Gp. **(b)** Mitochondrial respiration: The mitochondrial electron transfer system (ETS) is (***1***) fueled by diffusion and transport of substrates across the mitochondrial outer and inner membranes (mtOM and mtIM), and in addition consists of the (***2***) matrix-ETS, and (***3***) membrane-ETS. Electron transfer converges from dehydrogenases at the NADH-junction (N-junction), and from CI,

CII and electron transferring flavoprotein complex (CETF) at the Coenzyme Q-junction (Q-junction). Unlabeled arrows converging at the Q-junction indicate additional ETS-sections with electron entry into Q through Gp-dehydrogenase, dihydroorotate dehydrogenase, proline dehydrogenase, choline dehydrogenase, and sulfide-ubiquinone oxidoreductase. The dotted arrow indicates the branched pathway of oxygen consumption by alternative quinol oxidase (AOX). ET-pathways are coupled to the phosphorylation-pathway. The H^+_{pos}/O_2 ratio is the outward proton flux from the matrix space to the positively (pos) charged vesicular compartment, divided by catabolic O_2 flux in the NADH-pathway [26]. The $H^+_{neg}/P»$ ratio is the inward proton flux from the inter-membrane space to the negatively (neg) charged matrix space, divided by phosphorylation flux of ADP to ATP. These stoichiometries are not fixed because of ion leaks and proton slip. Modified from ref 27. **(c)** OXPHOS-coupling: The H^+ circuit couples O_2 flux through the catabolic ET-pathway, J_{kO_2}, to flux through the phosphorylation-pathway of ADP to ATP, $J_{P»}$. **(d)** Phosphorylation-pathway: the proton pump F_1F_O-ATPase (F-ATPase, ATP synthase), adenine nucleotide translocase (ANT), and inorganic phosphate carrier (PiC). The $H^+_{neg}/P»$ stoichiometry is the sum of the coupling stoichiometry in the F-ATPase reaction (-2.7 H^+_{pos} from the positive intermembrane space, 2.7 H^+_{neg} to the matrix, *i.e.*, the negative compartment) and the proton balance in the translocation of ADP^{3-}, ATP^{4-} and P_i^{2-} (negative for substrates) [12]. Modified from ref 8.

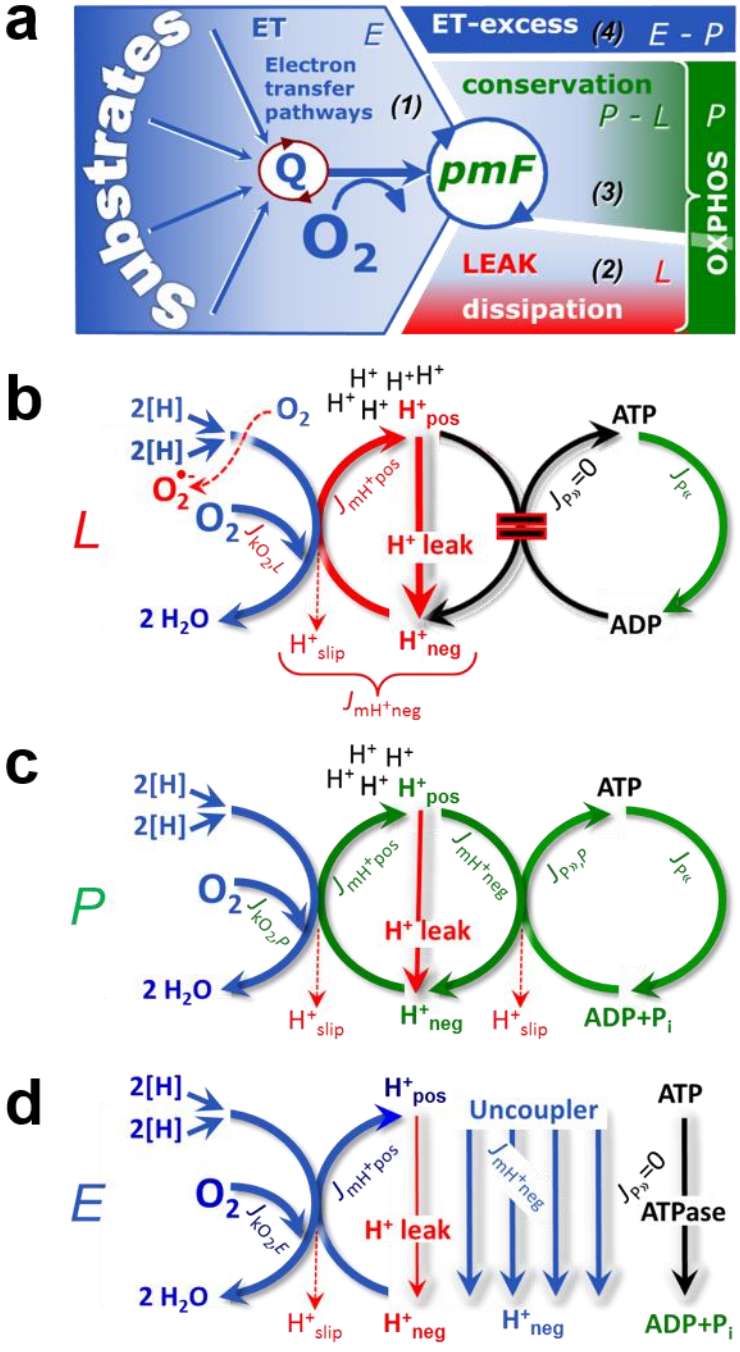

Fig. 2 | Respiratory states and rates. (a) Four-compartment model of oxidative phosphorylation: respiratory states (ET, OXPHOS, LEAK) and corresponding rates (*E*, *P*, *L*) are connected by the protonmotive force, *pmF*. (***1***) ET-capacity, *E*, is partitioned into (***2***) dissipative LEAK-respiration, *L*, when the Gibbs energy change of catabolic O_2 flux is irreversibly lost, (***3***) net OXPHOS-capacity, *P*-*L*, with partial conservation of the capacity to perform work, and (***4***) the ET-excess capacity, *E*-*P*. **(b) LEAK-rate, *L*:** Oxidation only, since phosphorylation is arrested, $J_{P»} = 0$, and catabolic O_2 flux, $J_{kO_2,L}$, is controlled mainly by the proton leak and slip, J_{mH^+neg} (motive, subscript m), at maximum protonmotive force. ATP may be hydrolyzed by ATPases, $J_{P«}$; then phosphorylation must be blocked. **(c) OXPHOS-rate, *P*:** Oxidation coupled to phosphorylation, $J_{P»}$, which is stimulated by kinetically-saturating [ADP] and [P_i], supported by a high protonmotive force maintained by pumping of protons to the positive compartment, J_{mH^+pos}. O_2 flux, $J_{kO_2,P}$, is well-coupled at a P»/O_2 flux ratio of $J_{P»,P}/J_{O_2,P}$. Extramitochondrial ATPases may recycle ATP, $J_{P«}$. **(d) ET- rate, *E*:** Oxidation only, since phosphorylation is zero, $J_{P»} = 0$, at optimum exogenous uncoupler concentration when noncoupled respiration, $J_{kO2,E}$, is maximum. The F_1F_O-ATPase may hydrolyze ATP entering the mitochondria. Modified from ref 8.

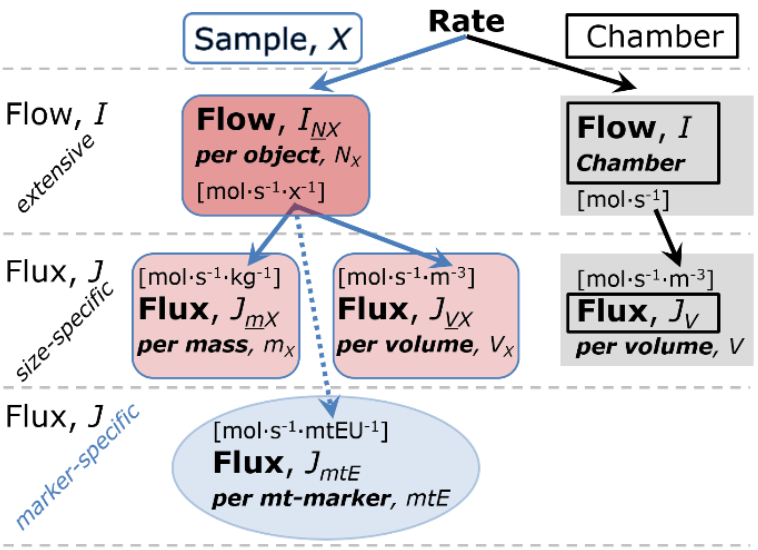

Fig. 3 | Different meanings of rate: flow and flux dependent on normalization for sample or instrumental chamber. Fundamental distinction between metabolic rate related to the experimental sample (left) or to the instrumental chamber (right). Left: Results are expressed as mass-specific *flux*, J_{mX}, per mg protein, dry or wet mass. Cell volume, V_{ce}, may be used for normalization (volume-specific flux, J_{Vce}). Normalization per mitochondrial elementary marker, *mtE*, relies on determination of mt-markers expressed in various mitochondrial elementary units [mtEU]. Right: Flow per instrumental chamber, I, or flux per chamber volume, J_V, are reported for methodological reasons.